



# Popeye: A Unified Visual-Language Model for Multi-Source Ship Detection from Remote Sensing Imagery

Wei Zhang, Miaoxin Cai, *Student Member, IEEE*, Tong Zhang, *Student Member, IEEE*, Guoqiang Lei, Yin Zhuang<sup>†</sup> *Member, IEEE*, and Xuerui Mao<sup>†</sup>

**Abstract**—Ship detection needs to identify ship locations from remote sensing (RS) scenes. However, due to different imaging payloads, various appearances of ships, and complicated background interference from the bird’s eye view, it is difficult to set up a unified paradigm for achieving multi-source ship detection. Therefore, in this article, considering that the large language models (LLMs) emerge the powerful generalization ability, a novel unified visual-language model called Popeye is proposed for multi-source ship detection from RS imagery. First, to bridge the interpretation gap between multi-source images for ship detection, a novel image-instruction-answer way is designed to integrate the various ship detection ways (e.g., horizontal bounding box (HBB), oriented bounding box (OBB)) into a unified labeling paradigm. Then, in view of this, a cross-modal image interpretation method is developed for the proposed Popeye to enhance interactive comprehension ability between visual and language content, which can be easily migrated into any multi-source ship detection task. Subsequently, owing to objective domain differences, a knowledge adaption mechanism is designed to adapt the pre-trained visual-language knowledge from the nature scene into the RS domain for multi-source ship detection. In addition, the segment anything model (SAM) is also seamlessly integrated into the proposed Popeye to achieve pixel-level ship segmentation without additional training costs. Finally, extensive experiments are conducted on the newly constructed instruction dataset named MMShip, and the results indicate that the proposed Popeye outperforms current specialist, open-vocabulary, and other visual-language models for zero-shot multi-source ship detection.

**Index Terms**—Visual-language alignment, ship detection, multi-source imagery, and natural language interaction.

## I. INTRODUCTION

SHIP detection in the present work refers to the technique to accurately identify ship locations from the remote sensing (RS) imagery with complex background interference [1]. Intelligent ship detection is critical for the analyses and

<sup>†</sup> Co-corresponding author: Yin Zhuang and Xuerui Mao.

Wei Zhang and Guoqiang Lei are with the Advanced Research Institute of Multidisciplinary Sciences, Beijing Institute of Technology, Beijing 100081, China, and also with the School of Mechatronical Engineering, Beijing Institute of Technology, Beijing 100081, China. (e-mail: w.w.zhanger@gmail.com, 3120235339@bit.edu.cn).

Xuerui Mao is with the Advanced Research Institute of Multidisciplinary Sciences, Beijing Institute of Technology, Beijing 100081, China, and with the School of Mechatronical Engineering, Beijing Institute of Technology, Beijing 100081, China, and also with Yangtze Delta Region Academy of Beijing Institute of Technology, Jiaxing 314003, China. (e-mail: xmao@bit.edu.cn).

Yin Zhuang, Miaoxin Cai, and Tong Zhang are with the National Key Laboratory of Science and Technology on Space-Born Intelligent Information Processing, Beijing Institute of Technology, Beijing 100081, China. (e-mail: yzhuang@bit.edu.cn, 3120220667@bit.edu.cn, bit\_zhangtong@163.com).

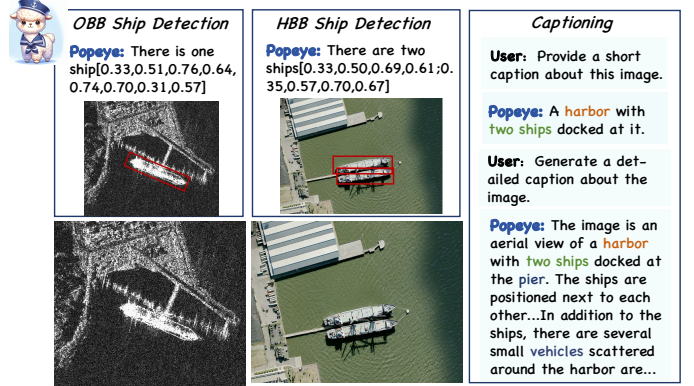


Fig. 1. Examples of multi-source (optical/SAR) ship image interpretation by the proposed Popeye, including ship detection via OBB or HBB, as well as image captioning.

monitoring of marine environments [2]. It is used in a wide range of fields such as maritime safety, border and territorial defense, naval warfare, environmental protection, search and rescue operations, maritime traffic control, and fishery management [3].

In the field of ship detection, many deep learning algorithms have been proposed. For the optical ship RS images analyses, the development of horizontal bounding box (HBB) detection methods, including CFF-SDN [4] and Li *et al.* [5], alongside oriented bounding box (OBB) detection methods such as RR-CNN [6] and Li *et al.* [7], has significantly improved the accuracy of optical ship detection. For synthetic aperture radar (SAR) ship image interpretation, many HBB algorithms such as CP-FCOS, etc. [8]–[12], as well as OBB ones including He *et al.* [13] and R-FCOS [14] have been proposed to enhance the performance of SAR ship detection. However, those are limited to handling individual detection tasks or single-source scenarios, rendering them incapable of uniformly interpreting multi-source ship images and performing multi-granularity detection within one framework, and subsequently constraining their applications to real-world problems. Therefore, this paper focuses on developing a novel unified ship interpretation framework for multi-source ship images, capable of both HBB, OBB detection, and segmentation.

Most recently, Large Language Models (LLMs) [15]–[17] have emerged as popular and innovative tools for human assistance, exhibiting robust generalization capabilities. Among

LLMs, a model named ChatGPT [18] stands out as a remarkable example, providing great potential for supporting humans in a diverse range of tasks. In addition, the considerable achievements of LLMs have sparked extensive research in introducing additional visual input and developing powerful multi-modal large language models (MLLMs) [19], [20]. Typically, studies such as MiniGPT-4 [21], LLaVA [22], and LLaMA-Adapter [23], [24] series have sparked a new wave of research on endowing LLMs with visual reasoning ability. The powerful capabilities of MLLMs have been demonstrated in various natural scenes. However, different from natural scene images, RS ones are gathered from an overhead view by satellites. Effectively adapting current MLLMs to the field of RS, and establishing a visual-language alignment paradigm for interpreting multi-source ship images presents significant challenges. To address these difficulties thoroughly, this work concentrates on constructing a unified visual-language framework to understand multi-source and multi-modal ship data in the RS domain.

In this paper, to exploit the powerful generalization ability of LLMs for developing a universal ship detection paradigm, a novel unified visual-language model named Popeye is proposed for multi-source ship interpretation in the RS domain. The proposed Popeye unifies various ship detection tasks and integrates multi-source imagery including optical and SAR in a naive visual-language alignment procedure. Firstly, to narrow the gap between the different RS visual modalities, a novel image-to-caption labeling approach is designed to unify the various ship detection formats. Utilizing the proposed unified labeling paradigm, a dataset named MMShip featuring multi-modal multi-source instruction-following is constructed based on existing ship detection datasets. Secondly, a suitable cross-modal image interpretation method is constructed, which can leverage language as a bridge to understand images. Given the RS imagery is complex and to enhance visual-language alignment efficacy, a hybrid visual feature extractor is developed to refine robust multi-scale visual representation, incorporating multiple pre-trained visual backbones, including CLIP ViT-L/14 [25] and DINOv2 ViT-L/14 [26]. Then, the visual features are concatenated with language features to form the multi-modal input. Subsequently, begin with a frozen LLaMA [16] model with superior resource efficiency and only insert the several Low-Rank Adaptation (LoRA) [27] metrics into LLaMA's higher Transformer layers for training. Through the aforementioned process, the language-only LLaMA is efficiently converted into a visual-language model by integrating visual information with the language instructions. Thirdly, a knowledge adaption paradigm for the ship domain is proposed [28], enabling the developed visual-language model to multi-source ship detection tasks. By continuing fine-tuning on the newly constructed MMShip dataset with the LoRA technique and the bias tuning strategy [24], Popeye successfully generalizes from the natural scene domain to the ship RS domain and achieves the multi-source detection ability. In addition, Popeye is integrated with the SAM [29] to extend language-guided ship segmentation capability without additional training costs. the proposed model can generate the accurate bounding boxes as the SAM prompt. In conclusion,

the proposed visual-language model Popeye can effectively unify ship HBB detection, OBB detection, captioning as well as segmentation, thereby meeting the requirements of multi-granularity detection (see the examples in Fig. 1).

Extensive experiments are conducted, demonstrating that Popeye has superior zero-shot performance on ship interpretation tasks compared to current specialist, open-vocabulary, and other visual-language models. For example, Popeye exhibits notable HBB detection improvements of 40.55%, 26.18%, and 4.16% on AP@40, AP@50, and AP@60 on the DSSDD dataset compared with the best results in other Visual-language Models and open-vocabulary models. For OBB detection, it is observed Popeye achieves improvements of 4.63% and 2.86% on AP@40 and AP@50 with Oriented R-CNN trained on DOTA. Therefore, Popeye significantly lowers the resource-intensive requirement of retraining on new data.

In summary, the main contributions of this paper are as follows.

- 1) To our best knowledge, the first unified visual-language model named Popeye is proposed for multi-source ship interpretation and multi-granularity ship detection tasks in a natural language interaction manner. In Popeye, the cross-modal image interpretation method enhances the mutual understanding of visual and language content effectively. Then, the knowledge adaptation mechanism migrates the visual-language model into the ship domain efficiently. Furthermore, Popeye's pixel-level segmentation ability is achieved by integrating it with the frozen SAM without additional training costs.
- 2) A unified labeling paradigm is proposed, converting various ship detection ways into the uniform image-instruction-answer data format, and the multi-source instruction dataset called MMShip is constructed for the first time. The MMShip, containing 81k instruction data, encompasses optical and SAR modalities, which is beneficial for the development of the ship generalist models by addressing the challenge posed by the scarcity of ship instruction datasets.
- 3) Extensive experiments demonstrate that Popeye excels in zero-shot ship HBB and OBB detection tasks, exceeding existing specialist, open-vocabulary, and other visual-language models. Moreover, Popeye shows excellent ship segmentation performance in challenging scenarios. Therefore, Popeye contributes a novel visual-language paradigm for diverse multi-source ship RS imagery interpretation tasks.

## II. RELATED WORK

### A. Large language models (LLMs)

In recent years, Natural Language Processing (NLP) has made significant progress, particularly with the advent of LLMs based on Transformer architectures. Among the LLMs, The GPT series [20], [25], [30] has gained considerable attention as a promising AI technique for NLP tasks. Especially GPT-3 [15], has demonstrated the power of massive model scaling, with models containing billions to trillions of parameters. InstructGPT [31] and ChatGPT [18] have shown

remarkable fluency and adaptability in various conversational tasks, which has improved their ability to follow instructions. Furthermore, the open-source community has contributed resources such as LLaMA [16] and LLaMA-2 [16], enriching the LLM’s instruction-following capability. Recent developments like Alpaca [32], Vicuna [33], and GPT-4-LLM [34] have proposed full fine-tuning to acquire the instruction-following ability of LLMs successfully. In contrast, LoRA [27] and LLaMA-Adapter [23] validate that parameter-efficient fine-tuning (PEFT) approaches can potentially replace full parameter updates during the supervised fine-tuning of LLMs. In this paper, Popeye is based on LLaMA-2’s language understanding and inspired by superior PEFT technique to fine-tune LLMs to achieve instruction-following ability with multi-modal input.

### B. Multi-modal large language models (MLLMs)

The fusion of LLMs and visual information revolutionizes image processing and unlock new practical applications in various fields. Previous efforts like the VisualGPT [35] and BLIP [36] series have demonstrated the possibilities of integrating LLMs with visual inputs, showcasing their effectiveness in tasks such as image captioning and visual question answering. Recently, GPT-4 [19] has showcased remarkable visual instruction-following abilities by handling visual-language inputs for multi-tasks. Moreover, Bard [37] also has demonstrated exceptional proficiency in multi-modal understanding and reasoning across diverse tasks. Concurrently, numerous works have focused on integrating LLaMA with the vision modality to enhance visual instruction-following capabilities. Models like LLaVA [22] and MiniGPT-4 [21] assemble high-quality multi-modal instruction-following data using ChatGPT or GPT-4. They employ a simple projection layer to integrate vision encoders with LLM and fine-tune the models on the curated data. The LLaMA-Adapter V2 [24] introduces zero-initialized attention mechanisms for efficient visual instruction tuning, while mPLUG-Owl [38] utilizes specially designed intermediate networks for effective cross-modal alignment. In this context, RS can directly benefit from MLLMs. Fine-tuned VLMs enable processing and analyzing satellite and aerial images. However, the application of generalized MLLMs in RS has been relatively limited. A notable attempt in this direction is RSGPT [39], which aimed to develop a model capable of tackling a variety of tasks. However, it is necessary to fine-tune RSGPT for individual tasks, which makes it a poor generalization performance. In the latest update, Geochat [40] has introduced a more integrated approach, intending to broaden the model’s capabilities to encompass regional-level analysis and visual grounding. Our Popeye aims to develop a parameter-efficient unified MLLM model to tackle the challenge of multi-task processing in ship RS understanding, using ship visual instruction-following data.

### C. Deep Learning based Ship Object Detection

Numerous algorithms based on deep learning have been proposed in the field of ship detection. High-performance RS object detectors often rely on the RCNN [41]–[43] framework, consisting of a region proposal network and regional

CNN detection heads. For the universal RS object detection, Variations like the RoI transformer [44] have been proposed, which leverages fully connected layers to rotate candidate horizontal anchor boxes before extracting features for regression and classification. Furthermore, AO2-DETR [45] introduces a transformer-based detection framework, which brings more research diversity. For the ship target detection from optical imagery, RR-CNN [6] is a rotated region based CNN method that can accurately extract features from rotated regions and precisely locate rotated objects. CFF-SDN [4] ship detection network uses multi-layer convolutional feature fusion to improve HBB high-precision ship detection. For the ship detection from SAR imagery, CP-FCOS [8] is an anchor-free method proposed for high-resolution SAR ship images. DAPN [8]. YOLOv2-reduced [12] architecture proposes an enhanced GPU-based deep learning method. In addition to image-level object detection, visual grounding is a region-level task, such as CLIP-VG [46] and RSVG [47] can locate the referred objects described by the language instruction, attracted much attention recently. However, Those algorithms are unable to uniformly understand multi-source ship images and complete both HBB and OBB ship detection tasks in one framework, which would constrain current intelligent interpretation methods for real-world applications. Therefore, this paper focuses on designing a unified multi-source ship RS image understanding framework, with a superior generalization capacity for cross-modal and multi-source image learning.

## III. METHOD

The overall architecture of the model Popeye is shown in Fig. 2. with the four main parts, (a) The unified labeling paradigm, (b) The cross-modal image interpretation method, (c) The knowledge adaption diagram, and (d) Integrated with SAM, addressed in section III-A, III-B, III-C and III-D, respectively. We will introduce each part in detail.

### A. Unified Labeling Paradigm

For developing a unified visual-language model for ship detection in the RS domain, it is essential to tackle the interpretation discrepancies across images from different RS visual modalities. To this end, a unified labeling paradigm is developed, as shown in Fig. 2 (a), utilizing the existing ship object detection datasets as the basic data to construct a new dataset named MMShip featuring multi-source multi-modal instruction-following. Specifically, four main ship detection datasets are considered, namely dataset DOSR [48] DOTA ship subset [49], SSDD [50], and HRSID [51]. Moreover, both the HBB and OBB detection ways are transformed into the uniform image-instruction-answer format.

During the conversion of datasets, specific language instructions are employed to direct the model towards predicting either HBB or OBB. For instance, for HBB detection, the model is instructed using the instruction, “Please detect all ships using the horizontal bounding box.”. Similarly, for OBB detection, the instruction is, “Please detect all ships using the oriented bounding box.”. Then, the formats of the answer are as follows: in the HBB format, a bounding box is defined by

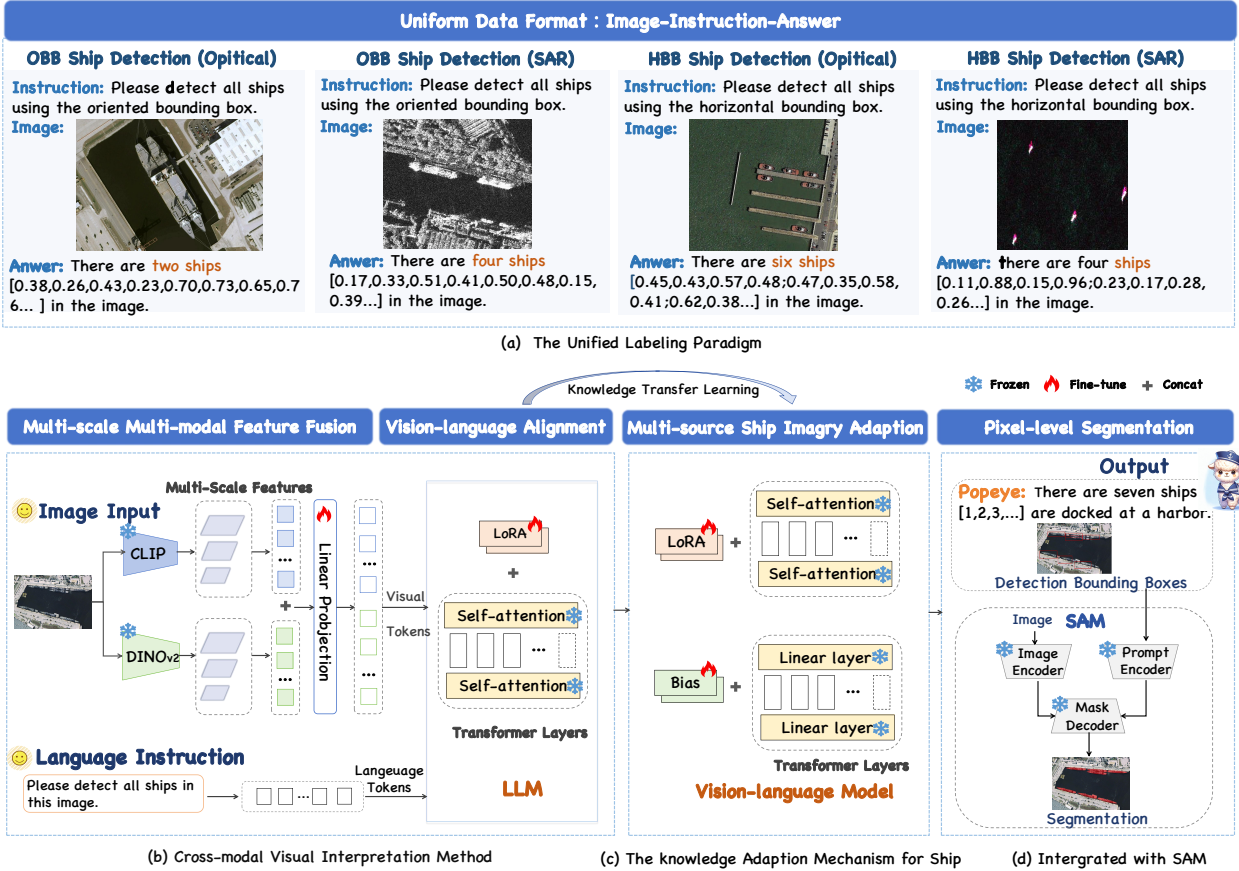


Fig. 2. The overall architecture of the proposed Popeye. (a) The unified data labeling paradigm to convert various ship detection ways to the uniform image-instruction-answer format. (b) The cross-modal image interpretation method includes a multi-scale multi-modal feature fusion module and a vision-language alignment tuning module. (c) The knowledge adaption mechanism for multi-source ship domain. (d) Integrated with the frozen SAM to extend language-guided pixel-level ship segmentation capability.

the coordinates  $[x_{\min}, y_{\min}, x_{\max}, y_{\max}]$ . The points  $(x_{\min}, y_{\min})$  and  $(x_{\max}, y_{\max})$  are identified as the corners of the bounding box that are, closest to and farthest from the origin of the coordinate system, respectively. Conversely, the OBB format is specified as  $[x_1, y_1, x_2, y_2, x_3, y_3, x_4, y_4]$ . Within this format, the point  $(x_1, y_1)$  is designated as the corner of the bounding box nearest to the coordinate origin, with the subsequent points  $(x_2, y_2)$ ,  $(x_3, y_3)$ , and  $(x_4, y_4)$  arranged in a sequence that ascends based on their angular relation to  $(x_1, y_1)$ . It is observed that in both HBB and OBB detection, the bounding box coordinates undergo a normalization process.

In conclusion, the MMShip dataset is constructed by assembling 81k instruction data of high-quality ship images. Leveraging the MMShip dataset can facilitate the evolution of the visual-language models for ship interpretation in the RS domain.

### B. Cross-modal Image Interpretation Method

Our goal in this part is to realize visual-language alignment to leverage language to facilitate image understanding. To this end, a multi-scale multi-modal fusion module and a visual-language alignment tuning module are proposed.

**Multi-scale Multi-modal Feature Fusion.** Given that ship RS images captured from an overhead perspective inherently

include complex background interference leads to significant challenges in accurately processing. To address this challenge and better utilize visual scale information, a multi-scale multi-modal feature fusion module is proposed. As depicted in Fig. 2 (b), various vision backbones are proposed for mixed image encoding, thereby achieving more robust visual representations. The CLIP ViT-L/14 [25] backbone is designed to extract multi-scale visual features from each input image  $I$ . Token embeddings generated by CLIP encoder denoted as  $\{f_v^i\}_{i=1}^n \in \mathbb{R}^{H \times W \times C}$ , where  $H \times W \times C$  represents the input image resolution,  $n$  is the scale number. Then the multi-scale feature is denoted as  $F_v$ . The entire process can be formulated as

$$f_v^i = \text{CLIP}_{\text{enc}}(I_i), \quad (1)$$

$$F_v = \text{Concat} [f_v^1, f_v^2, \dots, f_v^n]. \quad (2)$$

The DINOv2 ViT-L/14 [26] is further employed as another vision backbone to learn multi-scale visual tokens. Token embeddings generated by DINOv2 encoder is denoted as  $\{g_v^i\}_{i=1}^m \in \mathbb{R}^{H \times W \times C}$ , where  $m$  represents the scale number. Then the multi-scale feature is denoted as  $G_v$ . Similarly to the previous step, formulated as

$$g_v^i = \text{DINOv2}_{\text{enc}}(I_i), \quad (3)$$

$$G_v = \text{Concat} [g_v^1, g_v^2, \dots, g_v^m]. \quad (4)$$



Fig. 3. Examples of language-referred pixel-level segmentation by integrating Popeye and Segment Anything Model (SAM).

Then, the features extracted in the previous two steps are concatenated along the same channel dimension. Following that, a linear projection layer is used for dimension alignment with language tokens, and synthetical visual tokens are obtained and represented as  $p_v \in \mathbb{R}^{1 \times C}$ . The process can be expressed as

$$p_v = \text{Projection}(\text{Concat}[F_v, G_v]). \quad (5)$$

During the visual feature extraction process, the vision backbones are frozen to refine coarse-scale semantic information and fine-scale detail visual information. For language modality, the instructions are embedded as language tokens and denoted as  $p_l \in \mathbb{R}^{1 \times C}$ . By directly concatenating  $p_v$  and  $p_l$ , a multi-modal input  $\mathcal{X}$  is obtained. This process can be expressed as

$$\mathcal{X} = \text{Concat} \left[ \underbrace{[p_v^1, p_v^2, \dots, p_v^{N_v}]}_{\text{visual tokens } p_v}, \underbrace{[p_l^1, p_l^2, \dots, p_l^{N_l}]}_{\text{language tokens } p_l} \right], \quad (6)$$

where  $N_v$  represents the token length of visual features,  $N_l$  denotes the token length of language features,  $(p_v^1, p_v^2, \dots, p_v^{N_v})$  are the mixed visual backbone tokens from  $p_v$ , and  $(p_l^1, p_l^2, \dots, p_l^{N_l})$  are the language instruction tokens from  $p_l$ . At this stage, the visual and language information are integrated, forming the multi-modal input for the LLM.

**Visual-Language Alignment Tuning.** To endow the LLM with fundamental image understanding capability and realize visual-language alignment, the widely-used natural domain dataset COCO Caption [52] is employed for training. To avoid conventional expensive full-parameter fine-tuning and the risk of overfitting, the LoRA [27] technique which is a PEFT approach is adopted in this tuning stage. The LLaMA [16] is utilized as the LLM foundation model. The entire LLaMA weight matrices are frozen during training, and the learnable LoRA rank decomposition matrices are injected into

the topmost  $L$  layer of the Transformer architecture, greatly decreasing the number of trainable parameters for downstream tasks. The single attention matrix and multi-head attention of the  $l$ -th Transformer block can be computed as follows respectively

$$\text{Att}_l = \mathbf{W}_{Vl} \cdot \text{softmax} \left( \frac{\mathbf{W}_{Ql}(\mathbf{W}_{Kl})^T}{\sqrt{d_k}} \right), \quad (7)$$

$$\text{MultiAtt}_l = \sum_{h=1}^H \mathbf{W}_{Ol}^h \mathbf{W}_{Vl}^h \cdot \text{softmax} \left( \frac{\mathbf{W}_{Ql}^h (\mathbf{W}_{Kl}^h)^T}{\sqrt{d_k}} \right), \quad (8)$$

where  $H$  is the number of attention heads. The  $\mathbf{W}_{Ol}^h$ ,  $\mathbf{W}_{Ql}^h$ ,  $\mathbf{W}_{Kl}^h$ ,  $\mathbf{W}_{Vl}^h \in \mathbb{R}^{D \times D}$  are weight matrices for each attention head  $h \in H$  in the  $l$ -th Transformer block. In particular, four learnable low-rank adapter matrices  $\Delta \mathbf{W}_{Ql}^h, \Delta \mathbf{W}_{Kl}^h, \Delta \mathbf{W}_{Vl}^h, \Delta \mathbf{W}_{Ol}^h \in \mathbb{R}^{D \times D}$  are inserted into the topmost  $l$  layers of the Transformer architecture. The adapted multi-head attention is denoted as Adapted Attn, the output of the  $l$ -th adapted Transformer attention is defined as

$$\begin{aligned} \text{Adapted Attn}_l & \quad (9) \\ &= \sum_{h=1}^H (\mathbf{W}_{Ol}^h + \Delta \mathbf{W}_{Ol}^h) (\mathbf{W}_{Vl}^h + \Delta \mathbf{W}_{Vl}^h) \\ & \quad \times \text{softmax} \left( \frac{(\mathbf{W}_{Ql}^h + \Delta \mathbf{W}_{Ql}^h) (\mathbf{W}_{Kl}^h + \Delta \mathbf{W}_{Kl}^h)^T}{\sqrt{d_k}} \right). \end{aligned}$$

To sum up, this process begins with a frozen LLaMA as the starting point and refines it by optimizing the four smaller learnable matrices, achieving fundamental image captioning ability and enhancing the mutual understanding between images and language.

### C. Knowledge Adaption Mechanism for Ship Domain

With the methods documented in Section IV-A, a suitable visual-language alignment can be achieved. To further adapt to multi-source and multi-granularity detection ship tasks, continue fine-tuning the visual-language model on the newly constructed MMShip dataset.

To release the multi-source and cross-modal learning potential of LLM, more learnable parameters are added in the ship domain transfer learning stage, compared to the visual-language training one. As illustrated in Fig. 2 (c), Following LLaMA-Adapter V2 [24], the bias tuning strategy is also introduced alongside LoRA techniques during this stage. For each linear layer in the Transformer, a bias matrix  $\Delta W_b$  and a scale  $\Delta W_s$  factor are inserted as two trainable parameters. Given a linear layer  $f(x) = \mathbf{W}x$ , it can be transformed into

$$f(x) = \Delta \mathbf{W}_s(\mathbf{W}x + \Delta \mathbf{W}_b), \quad (10)$$

with learnable matrices  $\mathbf{W}$ ,  $\Delta \mathbf{W}_b$ , and  $\Delta \mathbf{W}_s \in \mathbb{R}^{D \times D}$ . The rest two are initialized with zeros and a random Gaussian, respectively, keeping fine-tuning stability and effectiveness. The mathematical formula can be expressed as  $\Delta \mathbf{W}_b = \text{Init}(0)$ ,  $\Delta \mathbf{W}_s \sim \mathcal{N}(\mu, \sigma^2)$ .

Distinct parameter optimization methods are adopted during the visual-language alignment and ship domain adaption stages. This separate optimization effectively addresses the challenges of interference between image-text understanding and the instruction-following ability, thereby enhancing the emergent ability of Popeye to follow language instructions to handle multi-source and multi-granularity ship detection tasks interactively.

### D. Integrated with SAM

In addition to ship detection capability, we also integrate the proposed Popeye with SAM [29] to tackle the more challenging language-referred pixel-level segmentation task. SAM is an open-ended image segmentation model that allows for promptable segmentation. However, ship images from RS imagery contain complex background interference and vague object edges, which affect SAM’s segmentation efficacy in this domain. The integration of our model with SAM enhances the capabilities of SAM specifically in the context of ship RS images. As illustrated in Fig. 2 (d), our Popeye can generate accurate ship HBB detection results based on the language instructions, and these results can be regarded as the prior prompts for SAM. Specifically, the SAM encoder uses the Masked Autoencoder (MAE) [53] to encode high-resolution image inputs into visual features and the bounding boxes generated from Popeye into the prompts embedding tokens. Then, the mask decoder efficiently enhances the interaction between image features and prompt embeddings, facilitating the generation of the mask output. The overall process [54] can be expressed as

$$F_{visual} = \text{SAM}_{v-enc}(I), \quad (11)$$

$$B_{det} = \text{Popeye}(I), \quad (12)$$

$$F_{prompt} = \text{SAM}_{p-enc}(B_{det}), \quad (13)$$

$$\Omega = \text{SAM}_{dec}(F_{visual}, F_{prompt}), \quad (14)$$

where  $I \in \mathbb{R}^{H \times W \times 3}$  represents the input image,  $F_{visual}$  refers to the visual features extracted by the SAM image encoder.  $B_{det}$  represents the sparse prompts including ship detection bounding boxes,  $F_{prompt}$  represents the sparse embedding tokens encoded by the prompt encoder and  $\Omega$  is the set of predicted masks.

In summary, the integration of Popeye with SAM enables an expansion of the language-guided ship segmentation at the pixel level, without additional training expenses. The proposed visual-language model Popeye can effectively unify ship HBB detection, ship OBB detection, and ship pixel-level segmentation tasks. Moreover, Popeye allows users to retrieve ship targets in RS images in a language-interactive manner. Fig. 3. shows examples of the applications for ship language-referred segmentation.

## IV. EXPERIMENTS

In this section, we conduct extensive experiments to validate the performance of the proposed Popeye. As mentioned in Section III, in the visual-language alignment stage, we start with a language-only LLM LLaMA and develop the multi-modal capabilities from scratch with common datasets. In the ship domain adaption stage, we continue tuning our model on the high-quality dataset MMShip to adapt for the ship domain. The datasets and the training configuration are detailed as follows.

### A. Implementation Details

**Datasets.** In the visual-language alignment stage, we train Popeye on COCO Caption [52], which are image captioning datasets in nature scenes. In the ship domain adaption phase, We further train on MMShip datasets to achieve ship HBB and OBB detection abilities. As mentioned in Section III, the MMShip dataset is constructed based on four different ship object detection datasets. Additionally, we have optimized the training procedure by converting all datasets into a unified conversation format. This not only reduces training costs but also boosts the overall efficiency.

**Settings.** In the visual-language alignment stage, we start with the off-the-shelf open-source weights LLaMA-7B [16] with 32 transformer layers and insert trainable LoRA matrices into the last  $L = 30$  transformers layers. The multiple visual encoders are kept frozen during the training. The visual projections are initialized randomly. We train our model using the AdamW optimizer [55] with a cosine learning rate scheduler. In the ship domain adaption stage, the optimizer settings are similar to the Pre-training stage. The trained and frozen parts remain the same as the visual-language alignment stage except the newly added bias and scale of the linear layer are learnable.

### B. Ship Object Detection

The evaluation of ship object detection is divided into HBB detection and OBB detection. To verify the potential of our proposed Popeye model in ship object HBB detection, we employ the zero-shot setting and compare Popeye with

other MLLMs and Open-vocabulary object detection models on three datasets including two optical ship detection datasets ShipRSImagenet, HRSC2016, and a SAR ship detection dataset DSSDD. To address the challenge of MLLMs not predicting confidence scores, we employ clip-score as a confidence logit. Remoteclip [56] weights are adopted to

compute the clipscore. For OBB detection, we adopt the OBB format of HRSC2016, DSSDD for zero-shot comparison with specialist models trained on DOTA. Additionally, the experiments mentioned above are conducted on the test set of the corresponding dataset.

As depicted in Tab. I, for HBB detection, Popeye exhibits

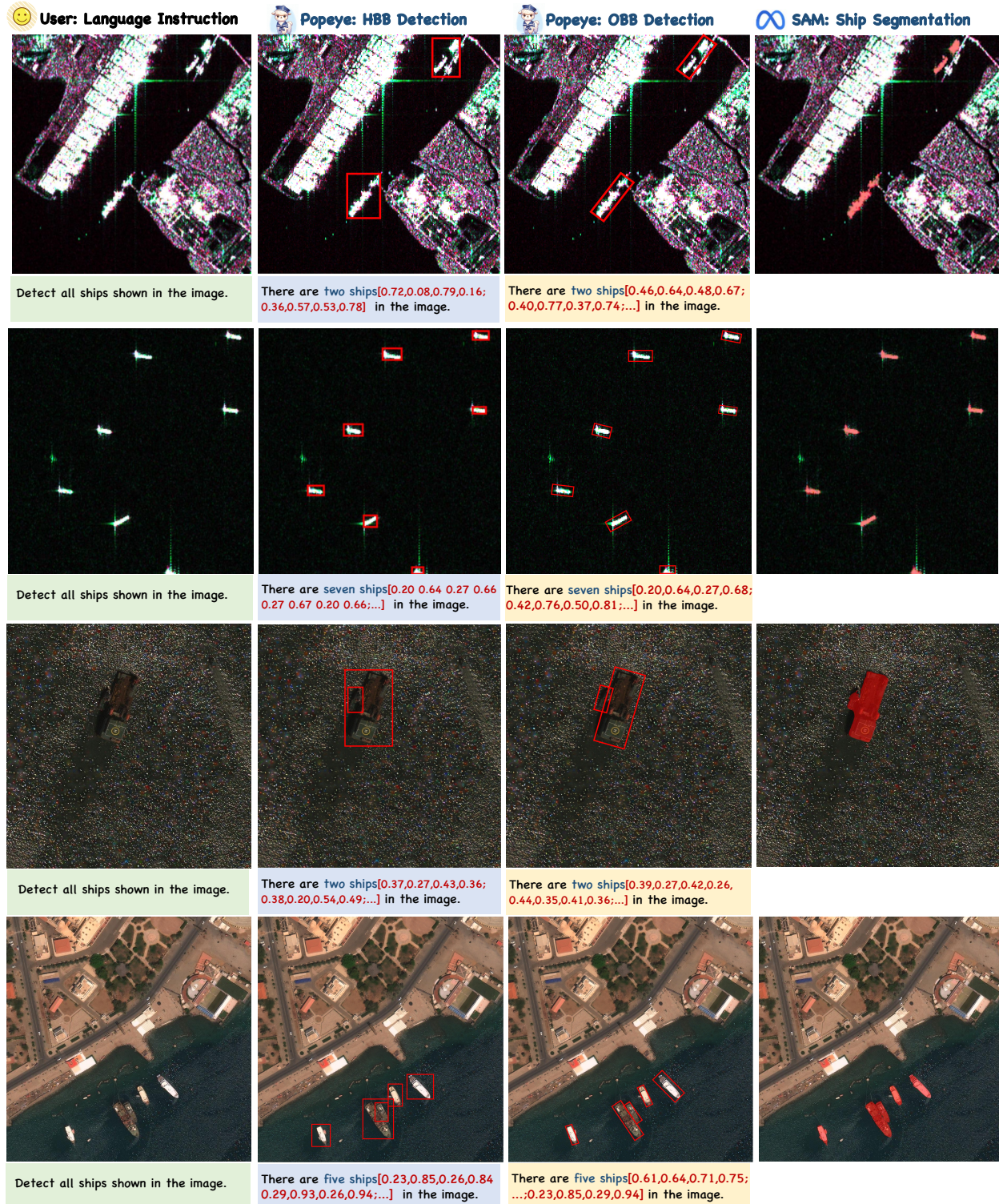


Fig. 4. Examples of Popeye for ships interpretation from more challenging SAR and optical RS imagery in ShipRSImagenet and DSSDD datasets. From left to right displays the results of Popeye for OBB detection, HBB detection, and ship instance segmentation of small and blurred ship targets.

TABLE I  
ZERO-SHOT COMPARISON RESULTS FOR HBB DETECTION ON SHIPRSIMAGENET FOR OTHER METHODS AND OUR METHOD POPEYE.

Method	Publication Year	AP@40	AP@50	AP@60
<i>Open-vocabulary Model</i>				
GroundingDINO [57]	Arxiv 2023	35.13	33.27	30.96
mm-GroundingDINO [58]	Arxiv 2024	38.19	37.18	35.57
<i>Visual-language Model</i>				
Lenna [59]	Arxiv 2023	49.27	47.41	44.51
Qwen-VL-Chat [60]	Arxiv 2023	30.34	22.69	21.32
Sphinx [61]	Arxiv 2023	41.61	40.82	40.70
<b>Popeye(Ours)</b>		<b>56.68</b>	<b>55.30</b>	<b>53.53</b>

TABLE II  
ZERO-SHOT COMPARISON RESULTS FOR HBB DETECTION ON DSSDD FOR OTHER METHODS AND OUR METHOD POPEYE.

Method	Publication Year	AP@40	AP@50	AP@60
<i>Open-vocabulary Model</i>				
GroundingDINO [57]	Arxiv 2023	22.31	20.24	14.68
mm-GroundingDINO [58]	Arxiv 2024	7.76	6.63	3.99
<i>Visual-language Model</i>				
Lenna [59]	Arxiv 2023	11.79	9.89	5.84
Qwen-VL-Chat [60]	Arxiv 2023	17.16	16.16	11.42
Sphinx [61]	Arxiv 2023	35.04	25.69	22.29
<b>Popeye(Ours)</b>		<b>75.59</b>	<b>51.87</b>	<b>26.45</b>

notable improvements of 7.41%, 7.89%, 9.02% on AP@40, AP@50, AP@60 when contrasted with other MLLMs and Open-vocabulary models on ShipRSimagenet. For the DSSDD dataset, when conducting HBB detection, Popeye brings improvements of 40.55%, 26.18%, 4.16% on AP@40, AP@50, and AP@60, compared with MLLM model Sphinx, which is shown in Tab. II. On the HRSC2016 dataset, Popeye suppresses the MLLM model Lenna with remarkable improvements of 13.31%, 7.35%, 6.51% on AP@40, AP@50 and AP@60. Comparative results on HRSC2016 are demonstrated on Tab. III. For OBB detection, it is observed from Tab. V that Popeye surpasses other specialist models trained on DOTA with the improvements of 4.63% and 2.86% on AP@40 and AP@50. Tab. IV also verifies that Popeye has a higher detection accuracy on HRSC2016 compared to other expert methods. These results demonstrate the potential and superiority of Popeye in ship target detection and also prove its powerful generalization ability in completely new, unseen environments. Furthermore, Fig. 4 provides a clear visualization of Popeye’s superior zero-shot detection accuracy in HBB and OBB formats.

### C. Ship Segmentation

We integrate Popeye with SAM to extend pixel-level segmentation capability. Popeye generates the horizontal bounding boxes for the ship target and serves as the prior prompts for SAM to achieve ship instance segmentation. We select

TABLE III  
ZERO-SHOT COMPARISON RESULTS FOR HBB DETECTION ON HRSC2016 FOR OTHER METHODS AND OUR METHOD POPEYE.

Method	Publication Year	AP@40	AP@50	AP@60
<i>Open-vocabulary Model</i>				
GroundingDINO [57]	Arxiv 2023	43.14	40.71	37.92
mm-GroundingDINO [58]	Arxiv 2024	48.47	47.59	46.12
<i>Visual-language Model</i>				
Lenna [59]	Arxiv 2023	57.05	55.14	52.05
Qwen-VL-Chat [60]	Arxiv 2023	39.23	30.21	22.39
Sphinx [61]	Arxiv 2023	56.11	55.32	54.38
<b>Popeye(Ours)</b>		<b>70.36</b>	<b>62.67</b>	<b>60.89</b>

TABLE IV  
ZERO-SHOT COMPARISON RESULTS FOR OBB DETECTION ON HRSC2016 FOR OTHER METHODS AND OUR METHOD POPEYE.

Method	Publication Year	AP@40	AP@50	AP@60
<i>Specialist Model</i>				
S2A-Net [62]	TGRS 2021	47.03	42.87	37.30
CFA [63]	CVPR 2021	47.62	44.97	39.55
Oriented RepPoints [64]	CVPR 2022	35.23	31.87	27.39
Oriented R-CNN [42]	ICCV 2021	52.99	51.79	<b>47.17</b>
Sasm [65]	AAAI 2022	31.45	28.27	25.14
R3Det [66]	AAAI 2021	36.11	30.76	24.20
<i>Visual-language Model</i>				
<b>Popeye(Ours)</b>		<b>58.15</b>	<b>54.91</b>	44.94

TABLE V  
ZERO-SHOT OBB DETECTION COMPARISON RESULTS FOR OBB DETECTION ON DSSDD FOR OTHER METHODS AND OUR METHOD POPEYE.

Method	Publication Year	AP@40	AP@50	AP@60
<i>Specialist Model</i>				
S2A-Net [62]	TGRS 2021	37.44	35.10	25.79
CFA [63]	CVPR 2021	30.44	24.62	16.76
Oriented RepPoints [64]	CVPR 2022	22.61	20.14	15.74
Oriented R-CNN [42]	ICCV 2021	17.34	16.92	15.81
R3Det [66]	AAAI 2021	58.49	49.05	30.35
<i>Visual-language Model</i>				
<b>Popeye(Ours)</b>		<b>63.12</b>	<b>51.92</b>	<b>38.35</b>

more challenging RS images of ships, including optical and SAR. These images are blurry to recognition, or the ships are camouflaged by the complex background or the ship targets are very tiny. In all these tested cases, we observe that the predicted segmentation masks for tiny and blurred ships are extremely accurate as shown in Fig. 4.

## V. CONCLUSION

In this paper, a unified visual-language Model called Popeye has been presented, excelling in uniformly handling multi-granularity ship detection tasks like HBB, OBB, pixel-level



ship segmentation, and captioning. Technically, a unified labeling paradigm has been developed to construct a dataset called MMSHIP, containing 81k multi-modal ship instruction-following data and covering multi-source RS images such as SAR and optical. Subsequently, a cross-modal image interpretation method and a knowledge adaption paradigm for the ship RS domain have been constructed, leveraging the language as a medium for bridging visual and language contexts and realizing a more universal paradigm for multi-source ship interpretation. In addition, Popeye is integrated with SAM to extend instance segmentation functionality without extra training expenses. Furthermore, we Extensive experiments have demonstrated that Popeye achieves robust zero-shot performances in multi-source ship imagery HBB detection, OBB detection, and pixel-level segmentation through natural language interactions.

## REFERENCES

- [1] LI Bo, XIE Xiaoyang, WEI Xingxing, and TANG Wenting. Ship detection and classification from optical remote sensing images: A survey. *Chinese Journal of Aeronautics*, 34(3):145–163, 2021.
- [2] Zongyong Cui, Qi Li, Zongjie Cao, and Nengyuan Liu. Dense attention pyramid networks for multi-scale ship detection in sar images. *IEEE Transactions on Geoscience and Remote Sensing*, 57(11):8983–8997, 2019.
- [3] Chao Dong, Jinghong Liu, and Fang Xu. Ship detection in optical remote sensing images based on saliency and a rotation-invariant descriptor. *Remote Sensing*, 10(3):400, 2018.
- [4] Yulian Zhang, Lihong Guo, Zengfa Wang, Yang Yu, Xinwei Liu, and Fang Xu. Intelligent ship detection in remote sensing images based on multi-layer convolutional feature fusion. *Remote Sensing*, 12(20):3316, 2020.
- [5] Linhao Li, Zhiqiang Zhou, Bo Wang, Lingjuan Miao, Zhe An, and Xiaowu Xiao. Domain adaptive ship detection in optical remote sensing images. *Remote Sensing*, 13(16):3168, 2021.
- [6] Zikun Liu, Jingao Hu, Lubin Weng, and Yiping Yang. Rotated region based cnn for ship detection. In *2017 IEEE International Conference on Image Processing (ICIP)*, pages 900–904. IEEE, 2017.
- [7] Linhao Li, Zhiqiang Zhou, Bo Wang, Lingjuan Miao, and Hua Zong. A novel cnn-based method for accurate ship detection in hr optical remote sensing images via rotated bounding box. *IEEE Transactions on Geoscience and Remote Sensing*, 59(1):686–699, 2020.
- [8] Zhongzhen Sun, Muchen Dai, Xiangguang Leng, Yu Lei, Boli Xiong, Kefeng Ji, and Gangyao Kuang. An anchor-free detection method for ship targets in high-resolution sar images. *IEEE Journal of Selected Topics in Applied Earth Observations and Remote Sensing*, 14:7799–7816, 2021.
- [9] Yuan Chen, Jie Yu, and Yang Xu. Sar ship target detection for ssdv2 under complex backgrounds. In *2020 International Conference on Computer Vision, Image and Deep Learning (CVIDL)*, pages 560–565. IEEE, 2020.
- [10] Mingming Zhu, Guoping Hu, Hao Zhou, Chunguang Lu, Yule Zhang, Shijie Yue, and Yao Li. Rapid ship detection in sar images based on yolov3. In *2020 5th international conference on communication, image and signal processing (CCISP)*, pages 214–218. IEEE, 2020.
- [11] Yan Zhao, Lingjun Zhao, Boli Xiong, and Gangyao Kuang. Attention receptive pyramid network for ship detection in sar images. *IEEE Journal of Selected Topics in Applied Earth Observations and Remote Sensing*, 13:2738–2756, 2020.
- [12] Yang-Lang Chang, Amare Anagaw, Lena Chang, Yi Chun Wang, Chih-Yu Hsiao, and Wei-Hong Lee. Ship detection based on yolov2 for sar imagery. *Remote Sensing*, 11(7):786, 2019.
- [13] Yishan He, Fei Gao, Jun Wang, Amir Hussain, Erfu Yang, and Huiyu Zhou. Learning polar encodings for arbitrary-oriented ship detection in sar images. *IEEE Journal of Selected Topics in Applied Earth Observations and Remote Sensing*, 14:3846–3859, 2021.
- [14] Xin Zhao, Bo Zhang, Zhixin Tian, Changgui Xu, Fan Wu, and Chunling Sun. An anchor-free method for arbitrary-oriented ship detection in sar images. In *2021 SAR in Big Data Era (BIGSAR DATA)*, pages 1–4. IEEE, 2021.
- [15] Tom Brown, Benjamin Mann, Nick Ryder, Melanie Subbiah, Jared D Kaplan, Prafulla Dhariwal, Arvind Neelakantan, Pranav Shyam, Girish Sastry, Amanda Askell, et al. Language models are few-shot learners. *Advances in neural information processing systems*, 33:1877–1901, 2020.
- [16] Hugo Touvron, Thibaut Lavril, Gautier Izacard, Xavier Martinet, Marie-Anne Lachaux, Timothée Lacroix, Baptiste Rozière, Naman Goyal, Eric Hambro, Faisal Azhar, et al. Llama: Open and efficient foundation language models. *arXiv preprint arXiv:2302.13971*, 2023.
- [17] Susan Zhang, Stephen Roller, Naman Goyal, Mikel Artetxe, Moya Chen, Shuohui Chen, Christopher Dewan, Mona Diab, Xian Li, Xi Victoria Lin, et al. Opt: Open pre-trained transformer language models. *arXiv preprint arXiv:2205.01068*, 2022.
- [18] OpenAI. Chatgpt. <https://chat.openai.com>, 2023a.
- [19] OpenAI. Gpt-4 technical report, 2023.
- [20] Alec Radford, Jeffrey Wu, Rewon Child, David Luan, Dario Amodei, Ilya Sutskever, et al. Language models are unsupervised multitask learners. *OpenAI blog*, 1(8):9, 2019.
- [21] Deyao Zhu, Jun Chen, Xiaoqian Shen, Xiang Li, and Mohamed Elhoseiny. Minigpt-4: Enhancing vision-language understanding with advanced large language models. *arXiv preprint arXiv:2304.10592*, 2023.
- [22] Haotian Liu, Chunyuan Li, Qingyang Wu, and Yong Jae Lee. Visual instruction tuning. *arXiv preprint arXiv:2304.08485*, 2023.
- [23] Renrui Zhang, Jiaming Han, Aojun Zhou, Xiangfei Hu, Shilin Yan, Pan Lu, Hongsheng Li, Peng Gao, and Yu Qiao. Llama-adapter: Efficient fine-tuning of language models with zero-init attention. *arXiv preprint arXiv:2303.16199*, 2023.
- [24] Peng Gao, Jiaming Han, Renrui Zhang, Ziyi Lin, Shijie Geng, Aojun Zhou, Wei Zhang, Pan Lu, Conghui He, Xiangyu Yue, et al. Llama-adapter v2: Parameter-efficient visual instruction model. *arXiv preprint arXiv:2304.15010*, 2023.
- [25] Alec Radford, Jong Wook Kim, Chris Hallacy, Aditya Ramesh, Gabriel Goh, Sandhini Agarwal, Girish Sastry, Amanda Askell, Pamela Mishkin, Jack Clark, et al. Learning transferable visual models from natural language supervision. In *International conference on machine learning*, pages 8748–8763. PMLR, 2021.
- [26] Maxime Oquab, Timothée Darcet, Théo Moutakanni, Huy Vo, Marc Szafraniec, Vasil Khalidov, Pierre Fernandez, Daniel Haziza, Francisco Massa, Alaaeldin El-Nouby, et al. Dinov2: Learning robust visual features without supervision. *arXiv preprint arXiv:2304.07193*, 2023.
- [27] Edward J Hu, Yelong Shen, Phillip Wallis, Zeyuan Allen-Zhu, Yuanzhi Li, Shean Wang, Lu Wang, and Weizhu Chen. Lora: Low-rank adaptation of large language models. *arXiv preprint arXiv:2106.09685*, 2021.
- [28] Tong Zhang, Peng Gao, Hao Dong, Yin Zhuang, Guanqun Wang, Wei Zhang, and He Chen. Consecutive pre-training: A knowledge transfer learning strategy with relevant unlabeled data for remote sensing domain. *Remote Sensing*, 14(22):5675, 2022.
- [29] Alexander Kirillov, Eric Mintun, Nikhila Ravi, Hanzi Mao, Chloe Rolland, Laura Gustafson, Tete Xiao, Spencer Whitehead, Alexander C Berg, Wan-Yen Lo, et al. Segment anything. *arXiv preprint arXiv:2304.02643*, 2023.
- [30] Alec Radford, Karthik Narasimhan, Tim Salimans, Ilya Sutskever, et al. Improving language understanding by generative pre-training. 2018.
- [31] Long Ouyang, Jeffrey Wu, Xu Jiang, Diogo Almeida, Carroll Wainwright, Pamela Mishkin, Chong Zhang, Sandhini Agarwal, Katarina Slama, Alex Ray, et al. Training language models to follow instructions with human feedback. *Advances in Neural Information Processing Systems*, 35:27730–27744, 2022.
- [32] Rohan Taori, Ishaan Gulrajani, Tianyi Zhang, Yann Dubois, Xuechen Li, Carlos Guestrin, Percy Liang, and Tatsunori B Hashimoto. Alpaca: A strong, replicable instruction-following model. *Stanford Center for Research on Foundation Models*. <https://crfm.stanford.edu/2023/03/13/alpaca.html>, 3(6):7, 2023.
- [33] Wei-Lin Chiang, Zhuohan Li, Zi Lin, Ying Sheng, Zhanghao Wu, Hao Zhang, Lianmin Zheng, Siyuan Zhuang, Yonghao Zhuang, Joseph E Gonzalez, et al. Vicuna: An open-source chatbot impressing gpt-4 with 90%\* chatgpt quality. See <https://vicuna.lmsys.org> (accessed 14 April 2023), 2023.
- [34] Baolin Peng, Chunyuan Li, Pengcheng He, Michel Galley, and Jianfeng Gao. Instruction tuning with gpt-4. *arXiv preprint arXiv:2304.03277*, 2023.
- [35] Jun Chen, Han Guo, Kai Yi, Boyang Li, and Mohamed Elhoseiny. Visualgpt: Data-efficient adaptation of pretrained language models for image captioning. In *Proceedings of the IEEE/CVF Conference on Computer Vision and Pattern Recognition*, pages 18030–18040, 2022.

- [36] Junnan Li, Dongxu Li, Caiming Xiong, and Steven Hoi. Blip: Bootstrapping language-image pre-training for unified vision-language understanding and generation. In *International Conference on Machine Learning*, pages 12888–12900. PMLR, 2022.
- [37] Google. Bard. <https://bard.google.com/>, 2023.
- [38] Qinghao Ye, Haiyang Xu, Guohai Xu, Jiabo Ye, Ming Yan, Yiyang Zhou, Junyang Wang, Anwen Hu, Pengcheng Shi, Yaya Shi, et al. mplug-owl: Modularization empowers large language models with multimodality. *arXiv preprint arXiv:2304.14178*, 2023.
- [39] Yuan Hu, Jianlong Yuan, Congcong Wen, Xiaonan Lu, and Xiang Li. Rsgpt: A remote sensing vision language model and benchmark. *arXiv preprint arXiv:2307.15266*, 2023.
- [40] Kartik Kuckreja, Muhammad Sohail Danish, Muzammal Naseer, Abhijit Das, Salman Khan, and Fahad Shahbaz Khan. Geochat: Grounded large vision-language model for remote sensing. *arXiv preprint arXiv:2311.15826*, 2023.
- [41] Ross Girshick, Jeff Donahue, Trevor Darrell, and Jitendra Malik. Rich feature hierarchies for accurate object detection and semantic segmentation. In *Proceedings of the IEEE conference on computer vision and pattern recognition*, pages 580–587, 2014.
- [42] Xingxing Xie, Gong Cheng, Jiabao Wang, Xiwen Yao, and Junwei Han. Oriented r-cnn for object detection. In *Proceedings of the IEEE/CVF international conference on computer vision*, pages 3520–3529, 2021.
- [43] Ross Girshick. Fast r-cnn. In *Proceedings of the IEEE international conference on computer vision*, pages 1440–1448, 2015.
- [44] Jian Ding, Nan Xue, Yang Long, Gui-Song Xia, and Qikai Lu. Learning roi transformer for oriented object detection in aerial images. In *Proceedings of the IEEE/CVF Conference on Computer Vision and Pattern Recognition*, pages 2849–2858, 2019.
- [45] Linhui Dai, Hong Liu, Hao Tang, Zhiwei Wu, and Pinhao Song. Ao2-detr: Arbitrary-oriented object detection transformer. *IEEE Transactions on Circuits and Systems for Video Technology*, 2022.
- [46] Linhui Xiao, Xiaoshan Yang, Fang Peng, Ming Yan, Yaowei Wang, and Changsheng Xu. Clip-vg: Self-paced curriculum adapting of clip via exploiting pseudo-language labels for visual grounding. *arXiv preprint arXiv:2305.08685*, 2023.
- [47] Yang Zhan, Zhitong Xiong, and Yuan Yuan. Rsvg: Exploring data and models for visual grounding on remote sensing data. *IEEE Transactions on Geoscience and Remote Sensing*, 61:1–13, 2023.
- [48] Yaqi Han, Xinyi Yang, Tian Pu, and Zhenming Peng. Fine-grained recognition for oriented ship against complex scenes in optical remote sensing images. *IEEE Transactions on Geoscience and Remote Sensing*, 60:1–18, 2021.
- [49] Jian Ding, Nan Xue, Gui-Song Xia, Xiang Bai, Wen Yang, Michael Yang, Serge Belongie, Jiebo Luo, Mihai Datcu, Marcello Pelillo, and Liangpei Zhang. Object detection in aerial images: A large-scale benchmark and challenges. *IEEE Transactions on Pattern Analysis and Machine Intelligence*, pages 1–1, 2021.
- [50] Tianwen Zhang, Xiaoling Zhang, Jianwei Li, Xiaowo Xu, Baoyou Wang, Xu Zhan, Yanqin Xu, Xiao Ke, Tianjiao Zeng, Hao Su, et al. Sar ship detection dataset (ssdd): Official release and comprehensive data analysis. *Remote Sensing*, 13(18):3690, 2021.
- [51] Shunjun Wei, Xiangfeng Zeng, Qizhe Qu, Mou Wang, Hao Su, and Jun Shi. Hrsid: A high-resolution sar images dataset for ship detection and instance segmentation. *Ieee Access*, 8:120234–120254, 2020.
- [52] Xinlei Chen, Hao Fang, Tsung-Yi Lin, Ramakrishna Vedantam, Saurabh Gupta, Piotr Dollár, and C Lawrence Zitnick. Microsoft coco captions: Data collection and evaluation server. *arXiv preprint arXiv:1504.00325*, 2015.
- [53] Kaiming He, Xinlei Chen, Saining Xie, Yanghao Li, Piotr Dollár, and Ross Girshick. Masked autoencoders are scalable vision learners. In *Proceedings of the IEEE/CVF conference on computer vision and pattern recognition*, pages 16000–16009, 2022.
- [54] Keyan Chen, Chenyang Liu, Hao Chen, Haotian Zhang, Wenyuan Li, Zhengxia Zou, and Zhenwei Shi. Rsprompter: Learning to prompt for remote sensing instance segmentation based on visual foundation model. *arXiv preprint arXiv:2306.16269*, 2023.
- [55] Diederik P Kingma and Jimmy Ba. Adam: A method for stochastic optimization. *arXiv preprint arXiv:1412.6980*, 2014.
- [56] Fan Liu, DeLong Chen, Zhangqingyun Guan, Xiaocong Zhou, Jiale Zhu, and Jun Zhou. Remoteclip: A vision language foundation model for remote sensing. *arXiv preprint arXiv:2306.11029*, 2023.
- [57] Shilong Liu, Zhaoyang Zeng, Tianhe Ren, Feng Li, Hao Zhang, Jie Yang, Chunyuan Li, Jianwei Yang, Hang Su, Jun Zhu, et al. Grounding dino: Marrying dino with grounded pre-training for open-set object detection. *arXiv preprint arXiv:2303.05499*, 2023.
- [58] Xiangyu Zhao, Yicheng Chen, Shilin Xu, Xiangtai Li, Xinjiang Wang, Yining Li, and Haian Huang. An open and comprehensive pipeline for unified object grounding and detection. *arXiv preprint arXiv:2401.02361*, 2024.
- [59] Fei Wei, Xinyu Zhang, Ailing Zhang, Bo Zhang, and Xiangxiang Chu. Lenna: Language enhanced reasoning detection assistant, 2023.
- [60] Jinze Bai, Shuai Bai, Shusheng Yang, Shijie Wang, Sinan Tan, Peng Wang, Junyang Lin, Chang Zhou, and Jingren Zhou. Qwen-vl: A frontier large vision-language model with versatile abilities. *arXiv preprint arXiv:2308.12966*, 2023.
- [61] Ziyi Lin, Chris Liu, Renrui Zhang, Peng Gao, Longtian Qiu, Han Xiao, Han Qiu, Chen Lin, Wenqi Shao, Keqin Chen, et al. Sphinx: The joint mixing of weights, tasks, and visual embeddings for multi-modal large language models. *arXiv preprint arXiv:2311.07575*, 2023.
- [62] Jiaming Han, Jian Ding, Jie Li, and Gui-Song Xia. Align deep features for oriented object detection. *IEEE Transactions on Geoscience and Remote Sensing*, 60:1–11, 2021.
- [63] Zonghao Guo, Chang Liu, Xiaosong Zhang, Jianbin Jiao, Xiangyang Ji, and Qixiang Ye. Beyond bounding-box: Convex-hull feature adaptation for oriented and densely packed object detection. In *Proceedings of the IEEE/CVF conference on Computer Vision and Pattern Recognition*, pages 8792–8801, 2021.
- [64] Wentong Li, Yijie Chen, Kaixuan Hu, and Jianke Zhu. Oriented reppoints for aerial object detection. In *Proceedings of the IEEE/CVF conference on computer vision and pattern recognition*, pages 1829–1838, 2022.
- [65] Liping Hou, Ke Lu, Jian Xue, and Yuqiu Li. Shape-adaptive selection and measurement for oriented object detection. In *Proceedings of the AAAI Conference on Artificial Intelligence*, 2022.
- [66] Xue Yang, Junchi Yan, Ziming Feng, and Tao He. R3det: Refined single-stage detector with feature refinement for rotating object. In *Proceedings of the AAAI Conference on Artificial Intelligence*, volume 35, pages 3163–3171, 2021.